Screen-Printed Chipless Wireless Temperature Sensor

Andreas Albrecht[1*], Jose F. Salmeron[1], Markus Becherer[1], Paolo Lugli[2], and Almudena Rivadeneyra[1]
[1]Institute for Nanoelectronics, Technical University of Munich, Munich, Germany
[2]Free University of Bozen-Bolzano, Bozen-Bolzano, Italy
*Email: andreas.albrecht@tum.de, almudena.rivadeneyra@tum.de

***Abstract*—A chipless wireless sensor for temperature monitoring is described in this work. The sensor is fabricated by screen printing of an RLC circuit on a flexible substrate. The sensing element is a resistive carbon paste with positive temperature coefficient placed in a small area in the interconnection between the inductor and the capacitor. This sensing layer modifies the resonance frequency of the circuit when the temperature varies. We also show the influence of the sensor sensitivity with respect to the reading distance.**

Keywords— coupling distance, flexible substrate, RLC circuit, resonance frequency

I. INTRODUCTION

Screen-printing is slowly being established as an alternative production method for electronic circuits for which low-power and low-energy consumption is required. The flexibility of the substrates, easy recyclability, low manufacturing cost as well as new design possibilities can change the way we use electronics today [1]. One eminent direction in electronics is the necessity to measure data in more and more locations of tiny devices (Internet of Things, IoT) and use machine learning algorithms to process the gathered data. Such node devices are typically equipped with a small or even no computing power. In contrast, the host systems can control many different nodes and possesses the main computing power of the system.

Most wireless sensing nodes are used in active mode and employ a small chip and a battery [2-4]. This requires additional components to be assembled on the device and increases complexity and dimensions of the node device. Typically, active devices deliver digital values about the measured parameters [5, 6]. Simple and completely passive wireless sensor nodes deliver analog values (voltage, time, frequency modulation among others) to the host system and, thus, move a substantial part of the computing power towards the host system. The larger the relation of the number of sensor nodes per host system the more favourable such a concentration of complexity in the host system is [7]. The major advantages lie in a much lower cost of passive devices compared to active ones and a lower power of the overall system [8]. Integrated Circuits (ICs), batteries, and energy harvesting are not necessary for passive, chipless tags and facilitate their production on flexible substrates. This production on flexible surfaces allows being attached to any object and, thus, facilitates the large-scale use of such sensor nodes, especially interesting for the Internet of Things (IoT) paradigm [9]. A major drawback can be the introduced noise on the transmitted analog values.

Radio Frequency Identification (RFID) antennas have been produced by means of printed electronics since many years for near field communication (NFC) as well as for higher frequencies and read ranges [10-12]. Printable, sensitive materials for many physical parameters have been developed and sensor solution developed. Among them, temperature sensors have been researched extensively and a large variety is available [13-15].

In this work we want to show a wireless temperature sensor that combines both, a chipless RF strategy with a fully screen-printed device. The sensor tag consists of a loop inductor and a capacitor that are connected in parallel to form a resonant circuit with a resonance frequency close to the NFC standard of 13.56 MHz. Both parts were screen-printed with silver paste. To achieve a temperature sensitivity, a short section of the connecting silver trace was replaced by a thick layer of positive temperature coefficient (PTC) paste that increases its resistance with increasing temperature.

II. MATERIALS AND METHODS

A. Pastes and fabrication process

The silver (Ag) screen printing paste employed in this work to print the antenna was LOCTITE ECI 1010 0.2KG E&C. The positive temperature coefficient (PTC) paste was LOCTITE ECI 8001 E&C [16]. These two pastes were provided by Henkel (Germany) and were used without modifications. The dielectric paste used to isolate the bridge connecting between the inner and outer inductor ends was TD-642 of AppliedInkSolutions (US).

All pastes were printed onto thermally pre-heated (100°C, 30 min) polyethylene terephthalate (PET) Melinex 506 of DuPont of a thickness of 100 µm. A manual screen printer (Siebdruck Versand) was used with a screen mesh density of 120 Threads/cm. After printing, the pastes were dried at 100°C for 30 min in an oven before printing the next type of paste.

B. Electrical characterization

The sheet resistances were measured with a constant DC current of 100 µA using a four-point probe head from Jandel connected to a Keysight B2901A source measuring unit.

The impedance change of the tag was measured with a Keysight E4990A Impedance Analyzer with an impedance

probe kit (42941A) for the sensor readout. The excitation voltage applied in all measurements was V_{DC} = 0 and V_{AC} = 500 mV and the frequency ranged from 8 MHz to 17 MHz. The measurements were automated with LabView 2016.

To conduct the temperature measurements, a VCL 4006 climate chamber of Vötsch (Germany) was used. A constant relative humidity of 60 % was fixed.

The distance between the reader and the sensors was defined with two rectangular spacers made of acrylonitrile butadiene styrene (ABS) with a perimeter of 85 mm x 53 mm manufactured with the 3D-printer EntresD UP Plus2. The height of the spaces was checked with a digital calliper (DIN 862) with a resolution of 0.01 mm.

III. Results and Discussion

A. PTC paste characterization

An SEM image of the PTC paste was taken and is shown in Figure 1. It shows small carbon particles that are embedded into a filler material. We assume that at a higher temperature this second component expands, which leads to a separation of the carbon particles and, thus, an increase in resistance as other works reported with other carbon-based sensitive pastes [17, 18].

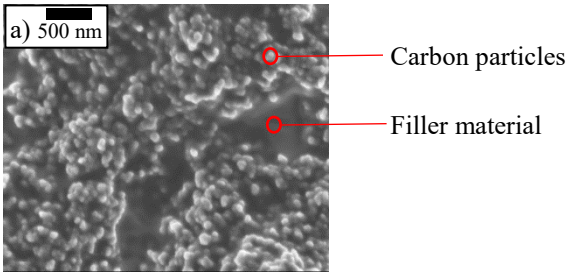

Figure 1. SEM image of the dried PTC paste with markers for the two main components

We investigated the properties of the plain PTC paste by printing a 5 x 5 cm² square with a mesh count of 120 T/cm, to deposit 15 µm thick layer onto a PET foil and measure the impedance across the square at different temperatures (15°C to 70°C in steps of 5°C). First, as can be seen in Fig. 2, the square can be modelled as a RC parallel circuit whose real part varies from R= 3 kΩ at 15 °C to R=4.57 kΩ at 55 °C with a parallel capacitor of only 4 pF insensitive to temperature. However, at temperatures upper 55 °C the electrical behaviour of the PTC paste changes abruptly. Resistance increase from 4.57 kΩ at 55°C to 30 kΩ at 70 °C whilst the modelled capacitance becomes 80 pF, so the PTC square behaves as a capacitor with a large ESR resistance. This is in accordance with the datasheet. In the following, we will distinguish between low temperatures that are below 55°C and high temperatures that are above 55°C due to the different behaviour of the PTC paste.

Figure 2 shows the impedance and phase values in the region that is relevant for our application in the high frequency range. It can be seen, that the impedance at 13.56 MHz depends almost linearly on the temperature and is about 1.5 kΩ. The phase component, however, shows a large difference between low temperatures (lower than 55 °C) and high temperatures (about 60°C and above) as explained.

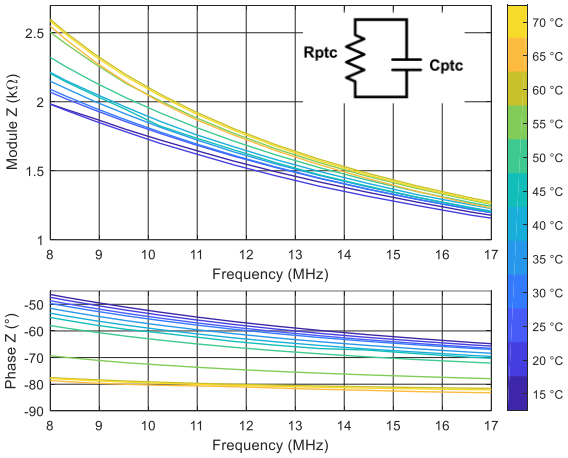

Figure 2. a) Absolute value and b) phase of the impedance of a square of the PTC paste at different temperatures

B. Sensor tag characterization

Figure 3 shows a photograph of the printed sensor tag. The inductor was printed with silver paste and the design was taken from [19] with only 4 turns. On the indicated dark area, the PTC paste was deposited. Figure 3 shows the complete systems including the tag in proximity of the reader antenna connected to the impedance analyzer. Coils of sensor and reader were aligned during measurements in order to maximize the coupling factor.

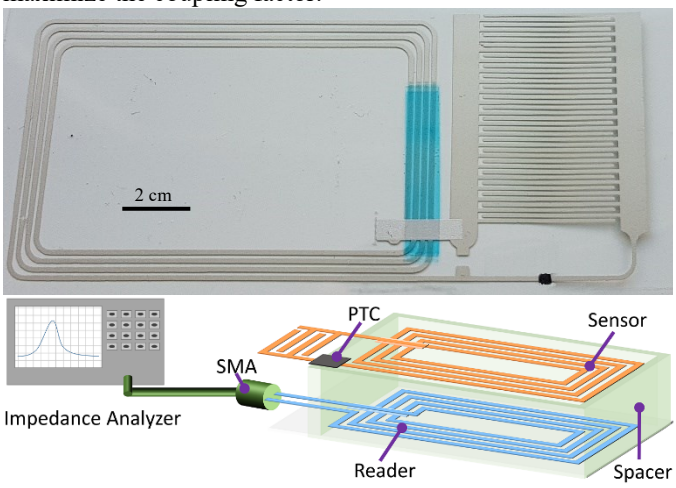

Figure 3. Photo of the tag (top) and system design (bottom)

The wireless temperature sensor tag consists of a silver-printed high frequency coil antenna connected to a co-planar printed capacitor that uses the PET film as a dielectric [20]. On a small section of only 1 mm of the interconnecting printed trace the silver was substituted by the PTC paste. The section is sufficiently small to avoid increasing the overall

resistance of the wire at low temperatures in order to not degrade antenna quality factor. At higher temperatures, the resistance of this section increases and dominates the resonant circuit.

The resonance frequency of a parallel LC resonant circuit with a resistor in series to the inductor can be modelled to equation 1.

$$□ = 2\pi \cdot \sqrt{\frac{1}{LC} - \left(\frac{R}{L}\right)^2} \qquad \text{Eq. 1}$$

The inductance L is mainly influenced by the coil wire forming the antenna for the electro-magnetic coupling and the capacitance C depends on the capacitance of the printed capacitor. The resistance R consists of two components, the resistance of the loop antenna and the resistance of the PTC paste. The later changes according to the temperature. An increase of the resistance in series to the inductor will reduce the resonance frequency. This frequency shift can be measured by an impedance analyser and should provide information about the current temperature.

An SMA (SubMiniature version A) male connector was glued at a suitable position on the connecting wires between coil antenna and capacitor using silver paint. The tag was characterized at varying temperatures and humidity in a climatic chamber. Figure 4 shows absolute value (a) and phase (b) over the frequency range from 8 MHz to 17 MHz for a selection of temperatures between 15°C and 70°C. Looking to the phase graph in Figure 4a and Figure 5 it is possible to better appreciate this abrupt response in temperature. The zero crossing of the phase is marked by filled circles in the phase plot. Figure 5 shows directly the measured resonance frequency versus temperature. At temperatures below 60°C the impedance curve peak constantly decreases and shifts to lower frequencies. For temperatures upper to 60 °C, the PTC sensor behaves as a series capacitance reducing the total capacitance shown in Equation 1 and causing an abrupt jump upwards in the impedance curve as shown in Figure 5. The resonance frequency decreases linearly by 11.4 ± 0.04 kHz/°C in the range from 15°C to 55°C (with a linear coefficient of 0.9964). A 95% confidence interval of sensitivity term was considered in the linear fit calculations. Then the increased resistance leads to an abrupt change in the resonance frequency. These results are in concordance with the temperature response of the PTC paste shown previously and with the datasheet of the manufacturer that claims a large resistance increase at 60°C.

It must be considered the effect against temperature of the single printed LC structure, without the PTC printed square. In a previous work [19], we studied the response at different temperatures of such silver screen-printed RLC circuits and we observed a variation of only 1.3 kHz in the range of 20 ºC to 55 ºC. Therefore, the insertion of the PTC in the RLC circuit provides 400 times higher change with temperature than the same device without this element.

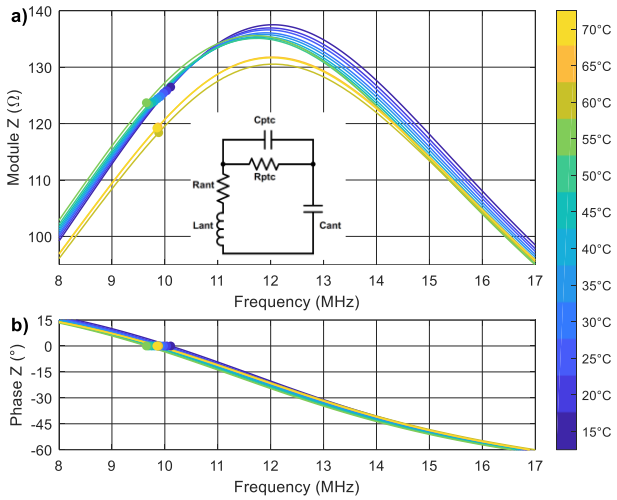

Figure 4. a) Absolute value and b) phase of impedance of the tag at 60% relative humidity at different temperatures. The impedance curve shifts towards lower frequencies with rising temperature from 15°C to 60°C. The phase shift reduces with increasing temperature. At higher temperatures (65°C and 70°C), the absolute impedance gets significantly lower and the phase flatter. The impedance and frequency at phase shift 0 is indicated by markers of the same colour.

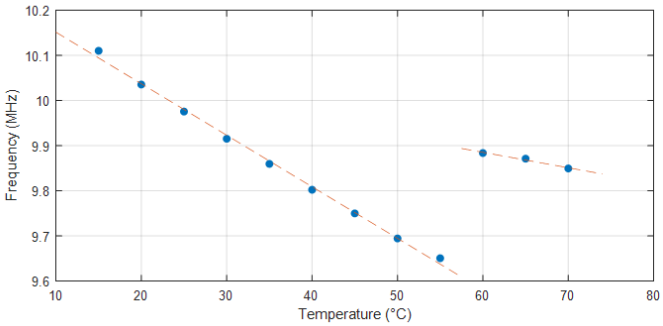

Figure 5. Change of resonance frequency measured on the tag with varying temperature with linear line fit. Errors were lower than 2% calculated as the standard deviation of 3 different cycles.

For varying humidity, the impedance remains almost constant over the entire range from 20% to 86% RH. In particular, the resonance frequency varies less than 150 Hz (0.001%) in the whole analysed RH range (Fig S1). This applies to both the absolute value and the phase within the measured range from 8 MHz to 17 MHz. Figure 6 shows the original measurement curves. Again, the impedance and frequency at the zero crossing of the phase are marked but almost perfectly overlap.

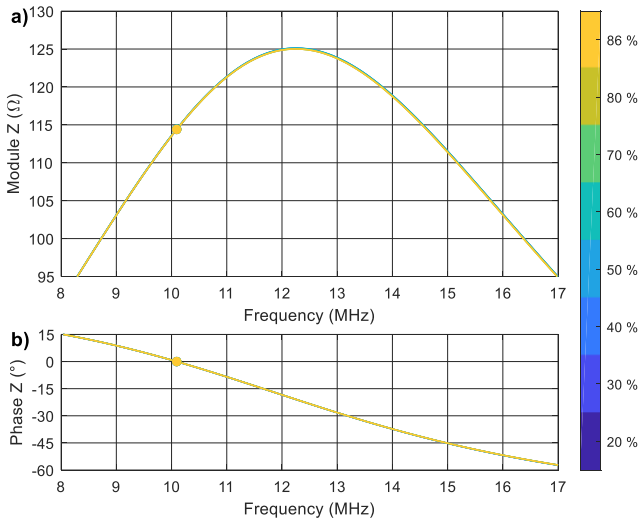

Figure 6. a) Absolute value and b) phase of impedance of the tag at 40°C at different humidity values. The impedance value is independent of the humidity. The impedance and frequency at phase shift 0 is indicated by markers of the same colour.

C. Wireless system characterization

In a second step, a copper coil antenna was used to couple to the wireless temperature sensor tag. The inductor consists of 7 turns enclosed in a rectangular area with height of 48 mm and width of 78 mm with both the line width and the gap of 600 µm. It was milled from a Flame-Retarded class 4 (FR-4) copper clad laminate rigid substrate with a 35 µm copper layer. A (SMD) capacitor was soldered to resonate at the desired frequency. The reader inductance value (L) is 5.99 µH. The inter-turn capacitance is 6.6 pF. A surface mount device (SMD) capacitor of 18 pF was soldered in parallel leading to a resonance frequency of 14.52 MHz. At a distance of 5 mm and 10 mm, the impedance spectrum was recorded. The original measurements showing amplitude and phase are provided in the supplementary information.

At a distance of 5 mm, a similar behaviour as the one measured directly on the sensor tag was found (see Fig S2). The resonance frequency decreases for temperatures below the abrupt change in conductivity/resistivity. A linear decrease of the frequency with the temperature of 3.3 ± 0.07 kHz/°C was found for the range below 55°C, with a linear coefficient of 0.9914. Above this value, the frequency increases again with a similar slope.

At a reading distance of 10 mm, however, we found that this increase does not occur anymore, and the resonance frequency decreases linearly with increasing temperature for the entire range. The slope is 1.8 ± 0.04 kHz/°C (with a linear coefficient of 0.9967) and considerably lower than for 5 mm distance. Figure 7 shows all interpolated frequencies at the zero-crossing of the phase for the temperature and humidity range at the two different distances to the reader.

For a varying humidity, the resonance frequency of the antenna at a distance of 5 mm remains mostly constant. This is in accordance previous published works [21] and shows that not even a higher water content of the substrate influences the coupling behaviour. The lower slope of the decrease of the resonance frequency at a distance of 10 mm in comparison to 5 mm can be explained by a lower coupling of the two antennas at a larger distance. At a larger distance or without the presence of the tag, no change in the resonance frequency of the reader antenna is expected and could be confirmed by measurements. Here, we do not observe the expected increase in the resonance frequency at 60°C because the coupling factor has decreased.

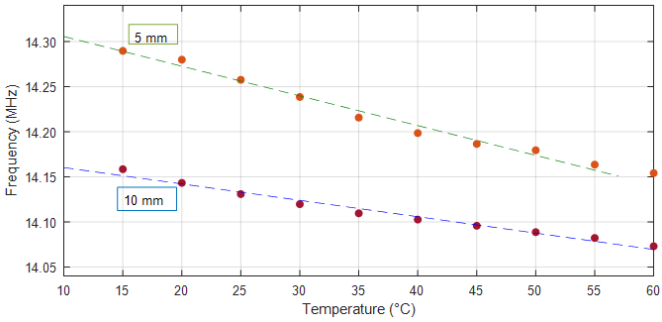

Figure 7. Resonance frequency measured on the reader antenna at different distance from the tag varying ambient temperature. Errors were lower than 2% calculated as the standard deviation of 3 different cycles.

Other authors have analysed wireless sensors for temperature monitoring, see Table 1. Although the linear response of our wireless sensor is constrained compared to other related works, the sensitivity achieved here is comparable and even higher than others. Furthermore, we have used a cost-effective technique both in terms of equipment and materials with lower costs than the ones used by other authors, being closer to a final sensor integrable, for example, in food industry.

TABLE 1. COMPARISON AMONG LC TYPE SENSOR FOR HUMIDITY MONITORING. *DISTANCE BETWEEN READER AND TAG ANTENNAS.

Ref.	Fabrication technology	Materials	Area (cm^2)	Sensitivity (kHz/ºC)	Temperature Range (ºC)	Distance* (mm)
Tan et al. 2015 [22]	Screen printing	Alumina based substrate Ag/Pd/Pt paste	8.4	-5.17	19-900	--
Tan et al. 2014 [23]	Screen printing	PbNb2O6-based ferroelectric ceramic Ag	3.7	-5.75 -16.67	25-430 430-700	--
Ren et al. 2015 [24]	Silicon-on-glass	Copper graphene oxide	0.04	-7.69	10-40	0.1-5
Yang et al. 2017 [25]	Screen printing	Aluminium nitride Ag/Pd paste	30.5	-104.77	25-700	15

This work	Screen printing	PET substrate Ag, Carbon PTC paste	40	-11.4 at 0 mm -1.8 at 10 mm	15-60	0-10

IV. Conclusion

In this work, we report on the design and characterization of screen printed chipless sensor for temperature monitoring. In particular, a silver RLC circuit is printed on a polymeric substrate and a small resistive carbon-based paste is defined in the connection between the other two circuit elements. This resistive element is a PTC, which influences the resonance characteristics of the RLC system. We found a sensitivity of 11.4 kHz/ºC at 0 mm and 1.8 kHz/ºC at 10 mm in the range of 15-60 ºC. This kind of sensing device will be very useful for the development of cost-effective and flexible devices to monitor environmental parameters, especially interesting for the Internet of Things paradigm.

Acknowledgment

This work was partially supported by the TUM Graduate School. This work has been also supported by the fellowship H2020-MSCA-IF-2017-794885-SELFSENS.

References

[1] S. Khan, L. Lorenzelli, and R. S. Dahiya, "Technologies for printing sensors and electronics over large flexible substrates: a review," *IEEE Sensors Journal,* vol. 15, pp. 3164-3185, 2015.

[2] R. Vyas, V. Lakafosis, A. Rida, N. Chaisilwattana, S. Travis, J. Pan*, et al.*, "based RFID-enabled wireless platforms for sensing applications," *IEEE Transactions on Microwave Theory and Techniques,* vol. 57, pp. 1370-1382, 2009.

[3] S. Veerasingam, S. Karodi, S. Shukla, and M. C. Yeleti, "Design of wireless sensor network node on ZigBee for temperature monitoring," in *Advances in Computing, Control, & Telecommunication Technologies, 2009. ACT'09. International Conference on*, 2009, pp. 20-23.

[4] K. Opasjumruskit, T. Thanthipwan, O. Sathusen, P. Sirinamarattana, P. Gadmanee, E. Pootarapan*, et al.*, "Self-powered wireless temperature sensors exploit RFID technology," *IEEE Pervasive computing,* pp. 54-61, 2006.

[5] A. Georgiadis, A. Collado, S. Via, and C. Meneses, "Flexible hybrid solar/EM energy harvester for autonomous sensors," in *Microwave Symposium Digest (MTT), 2011 IEEE MTT-S International*, 2011, pp. 1-4.

[6] Z. Fan, R. X. Gao, and D. O. Kazmer, "Design of a self-energized wireless sensor for simultaneous pressure and temperature measurement," *Advanced Intelligent Mechatronics (AIM),* 2010.

[7] D. Girbau, Á. Ramos, A. Lazaro, S. Rima, and R. Villarino, "Passive wireless temperature sensor based on time-coded UWB chipless RFID tags," *IEEE Transactions on Microwave Theory and Techniques,* vol. 60, pp. 3623-3632, 2012.

[8] R. Bhattacharyya, C. Floerkemeier, and S. Sarma, "Low-cost, ubiquitous RFID-tag-antenna-based sensing," *Proceedings of the IEEE,* vol. 98, pp. 1593-1600, 2010.

[9] R. Colella, A. Rivadeneyra, A. J. Palma, L. Tarricone, L. F. Capitan-Vallvey, L. Catarinucci*, et al.*, "Comparison of Fabrication Techniques for Flexible UHF RFID Tag Antennas [Wireless Corner]," *IEEE Antennas and Propagation Magazine,* vol. 59, pp. 159-168, 2017.

[10] J. F. Salmerón, F. Molina-Lopez, A. Rivadeneyra, A. V. Quintero, L. F. Capitán-Vallvey, N. F. d. Rooij*, et al.*, "Design and development of sensing RFID Tags on flexible foil compatible with EPC Gen 2," *IEEE Sensors,* vol. 14, pp. 4361 - 4371, 2014.

[11] J. Fernandez-Salmeron, A. Rivadeneyra, M. A. Carvajal Rodriguez, L. F. Capitan-Vallvey, and A. J. Palma, "HF RFID Tag as Humidity Sensor: Two Different Approaches," *Sensors Journal, IEEE,* vol. 15, pp. 5726-5733, 2015.

[12] A. Blayo and B. Pineaux, "Printing processes and their potential for RFID printing," in *Proceedings of the 2005 joint conference on Smart objects and ambient intelligence: innovative context-aware services: usages and technologies*, 2005, pp. 27-30.

[13] J. Courbat, Y. Kim, D. Briand, and N. de Rooij, "Inkjet printing on paper for the realization of humidity and temperature sensors," in *Solid-State Sensors, Actuators and Microsystems Conference (TRANSDUCERS), 2011 16th International*, 2011, pp. 1356-1359.

[14] S. Harada, K. Kanao, Y. Yamamoto, T. Arie, S. Akita, and K. Takei, "Fully printed flexible fingerprint-like three-axis tactile and slip force and temperature sensors for artificial skin," *ACS nano,* vol. 8, pp. 12851-12857, 2014.

[15] A. Albrecht, A. Rivadeneyra, M. Bobinger, J. B. Calia, F. C. Loghin, J. F. Salmeron*, et al.*, "Scalable Deposition of Nanomaterial-Based Temperature Sensors for Transparent and Pervasive Electronics," *Journal of Sensors,* vol. 2018, 2018.

[16] LOCTITE. (2017, 06 Nov 2018). *LOCTITE ECI 8001 E&C*. Available: https://tdsna.henkel.com/NA/UT/HNAUTTDS.nsf/web/8839A5D0F3CA28C085257B2600747FB5/$File/42720466.PDF

[17] M. C. Lonergan, E. J. Severin, B. J. Doleman, S. A. Beaber, R. H. Grubbs, and N. S. Lewis, "Array-based vapor sensing using chemically sensitive, carbon black-polymer resistors," *Chemistry of Materials,* vol. 8, pp. 2298-2312, 1996.

[18] A. Rivadeneyra, J. Fernández-Salmerón, M. Agudo-Acemel, J. A. López-Villanueva, L. F. Capitán-Vallvey, and A. J. Palma, "Hybrid Printed Device for

Simultaneous Vapors Sensing," *IEEE Sensors Journal,* vol. 16, pp. 8501-8508, 2016.

[19] J. Fernández-Salmerón, A. Rivadeneyra, M. A. C. Rodríguez, L. F. Capitan-Vallvey, and A. J. Palma, "HF RFID tag as humidity sensor: Two different approaches," *IEEE Sensors Journal,* vol. 15, pp. 5726-5733, 2015.

[20] A. Rivadeneyra, J. F. Salmerón, M. Agudo-Acemel, L. F. Capitan-Vallvey, J. A. López-Villanueva, and A. J. Palma, "Asymmetric enhanced surface interdigitated electrode capacitor with two out-of-plane electrodes," *Sensors and Actuators B: Chemical,* vol. 254, pp. 588-596, 2018.

[21] J. Salmerón, A. Albrecht, S. Kaffah, M. Becherer, P. Lugli, and A. Rivadeneyra, "Wireless Chipless System for Humidity Sensing," *Sensors,* vol. 18, p. 2275, 2018.

[22] Q. Tan, Z. Ren, T. Cai, C. Li, T. Zheng, S. Li*, et al.*, "Wireless passive temperature sensor realized on multilayer HTCC tapes for harsh environment," *Journal of Sensors,* vol. 2015, 2015.

[23] Q. Tan, T. Luo, J. Xiong, H. Kang, X. Ji, Y. Zhang*, et al.*, "A harsh environment-oriented wireless passive temperature sensor realized by LTCC technology," *Sensors,* vol. 14, pp. 4154-4166, 2014.

[24] Q.-Y. Ren, L.-F. Wang, J.-Q. Huang, C. Zhang, and Q.-A. Huang, "Simultaneous remote sensing of temperature and humidity by LC-type passive wireless sensors," *Journal of Microelectromechanical Systems,* vol. 24, pp. 1117-1123, 2015.

[25] D. Yan, Y. Yang, Y. Hong, T. Liang, Z. Yao, X. Chen*, et al.*, "AlN-Based Ceramic Patch Antenna-Type Wireless Passive High-Temperature Sensor," *Micromachines,* vol. 8, p. 301, 2017.